ELSEVIER

Polymer 41 (2000) 7263–7271

polymer

Absorption of low molecular weight penetrants by a thermoplastic polyimide

A.A. Goodwin[1,a,*], A.K. Whittaker[b], K.S. Jack[b], J.N. Hay[c], J. Forsythe[a]

[a]*Materials Engineering, Monash University, Clayton 3168, Victoria, Australia*
[b]*Centre for Magnetic Resonance, University of Queensland, Queensland 4072, Australia*
[c]*Metallurgy and Materials, Birmingham University, Birmingham B15 2TT, UK*

Received 2 June 1999; received in revised form 7 September 1999; accepted 12 January 2000

Abstract

The response of a thermoplastic polyimide (TPI) to immersion in a range of solvents was investigated by a number of experimental techniques. The kinetics of solvent diffusion were determined by weight uptake and NMR imaging, the effect of absorbed solvent on thermal behaviour was investigated by dynamic mechanical analysis and differential scanning calorimetry and the morphology of TPI exposed to solvent was determined by wide-angle X-ray scattering. The tensile properties of amorphous and crystalline TPI were measured before and after exposure to solvent. Amorphous TPI absorbed significant quantities of some solvents that lowered the T_g, but none were sufficiently plasticising to induce crystallisation at room temperature. There was a direct correlation between the extent of solvent ingress and the environmental stress cracking behaviour of amorphous TPI. Crystalline TPI absorbed only small quantities of all the solvents used, but showed limited environmental stress cracking resistance.

Keywords: Thermoplastic polyimide; Diffusion; Nuclear magnetic resonance

1. Introduction

High performance polyimides are used across a broad range of engineering applications. The presence of aromatic and imide groups in the monomer unit impart rigidity and strong interchain interactions to the polymer, and thus result in high thermal stability and good mechanical properties. Polyimides can also be designed with a low dielectric constant that makes them suitable for use as insulation in electrical and electronic applications. The development of a new thermoplastic polyimide (TPI) based on the monomers pyromellitic dianhydride and 3,3′-bis (4-aminophenoxy) biphenyl diamine has been the subject of investigation for a number of research groups [1–3], and the crystal structure, morphology, thermal and crystallisation behaviour and relaxation behaviour have been reported. This polymer, the structure of which is shown below,

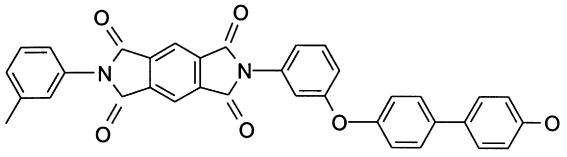

contains flexible ether and *meta*-phenyl linkages, which allow the polymer to be processed by conventional thermoplastic melt-processing techniques. The amorphous material has a T_g around 250°C and, in the crystalline form, has an experimental melting temperature of about 385°C.

The majority of gravimetric studies concerned with the diffusion of solvents into advanced thermoplastics have focussed on poly (ether ether ketone) (PEEK), a semi-crystalline material in which the degree of crystallinity can be controlled by thermal history. Although the chemical resistance of semi-crystalline PEEK is excellent, the amorphous polymer absorbs significant amounts of benzene derivatives and chlorinated hydrocarbons that cause plasticisation and subsequent solvent-induced crystallisation. Environmental stress cracking (ESC) of polymers is a general term that is used to describe the crazing which occurs under stress and is promoted by liquid or gas. ESC agents are thought to promote crazing in polymers by decreasing the surface energy and plasticising the matrix [4].

* Corresponding author. Tel.: + 61-3-9214-2174; fax: + 61-3-9646-7339.

E-mail address: andy.goodwin@boral.com.au (A.A. Goodwin).

[1] Current address: Boral Plasterboard, 676 Lorimer Street, Port Melbourne, Victoria 3207, Australia.

0032-3861/00/$ - see front matter
PII: S0032-3861(00)00063-X

Numerous examples of the application of NMR imaging to the study of ingress of solvents into polymers can be found in the literature. Early studies concentrated on the ingress of organic solvents, namely methanol and acetone into poly (methyl methacrylate) [5–9], and this work has been recently extended over a range of temperature up to 60°C [10]. At ambient temperature the diffusion mechanism can be characterised from the form of the diffusion front as obeying Case II kinetics [5–10], while at higher temperatures the diffusion tends towards Fickian kinetics [10]. The transition to Fickian kinetics occurs at a temperature close to the glass transition temperature of the polymer/solvent mixture. Such an observation agrees well with observed Fickian diffusion of acetone and benzene in natural rubber samples [11–13]. The advantage of NMR imaging over less direct methods of studying ingress of solvents is the possibility to observe evidence of anomalous diffusion. For example, the kinetics of increase of mass of water in poly (hydroxyethyl methacrylate-*co*-tetrahydrofurfuryl methacrylate) has been shown to obey Fick's laws up to moderate diffusion times [14]. However, NMR images [14] of water within these copolymers over the same times shows the presence of an anomalous feature, which is assigned to water in cracks near the boundary of the swollen rubbery polymer and the glassy inner core. The T_2 relaxation time of the water protons within the cracks is significantly longer than that of water closely associated with the polymer chains.

The ingress of solvents into a range of other polymers has also been studied, including organic solvents into glassy [15–17] and semicrystalline materials [18,19], water into nylon and relatively hydrophobic polymers. A number of recent studies have dealt with transport of water in hydrogels of interest for biomedical applications [18].

In this paper, we report the chemical resistance and mechanical behaviour of a thermoplastic polyimide when exposed to the solvents chloroform, dichloromethane, acetone, toluene and 1,1,2,2-tetrachloroethane (TCE). These solvents were chosen for their different solubility parameters and their common use in industrial environments. Solvent uptake was followed using gravimetric and nuclear magnetic resonance (NMR) techniques, solvent plasticisation was observed with dynamic mechanical analysis (DMA), while wide-angle X-ray scattering (WAXS) and differential scanning calorimetry (DSC) were used to check for solvent-induced crystallisation. Mechanical behaviour of the polymer when exposed to solvents was also investigated.

2. Experimental

2.1. Materials

TPI (Aurum 450) with $M_w = 27\,000$ g/mol was supplied by Mitsui Toatsu Chemical Co. Specimens were compression moulded at 400°C and then quenched into iced water to form amorphous sheets. Semi-crystalline specimens were prepared by annealing amorphous sheets at 290°C for 2 h. The degree of crystallinity of thermally crystallised specimens was determined by DSC and was 27%. Solvents used in the diffusion studies were standard laboratory reagents.

2.2. Weight uptake

Specimens of 0.5 mm thickness were immersed in solvent in sealed containers at room temperature. They were removed at periodic intervals and quickly weighed to determine the weight change, before re-immersion in solvent. This procedure was repeated until equilibrium was reached.

2.3. Nuclear magnetic resonance

NMR images were performed on an AMX300 spectrometer equipped with a Bruker micro-imaging gradient set and 5 mm birdcage resonator probe. The 1.8 mm thick specimen was removed from the acetone after a certain period, and fixed securely in a 5 mm NMR tube. The spin-echo 3D sequence was used to acquire the images, which were zero-filled to 256×256 points in plane over 2.53 mm. This is a pixel size of 10×10 μm and the resolution is therefore 20 μm with a slice thickness of 300 μm. Images were collected using different echo times to confirm that the spin–spin relaxation time did not vary across the diameter of the film, as observed for other materials [14].

The echo time was 3.1 ms, the $\pi/2$ pulse time was 9 μs and the pulse repetition time was 1 s. A total of two averages were co-added to achieve a satisfactory signal-to-noise ratio, resulting in a total experiment time of 34 min. The total imaging time of 34 min was small compared with the time to achieve equilibrium, and so it was considered that the solvent front was stationary during the measurement. Collecting an image a second time immediately after the first image and comparing the form of the solvent front in the two images confirmed this. In addition, the sample was weighed before and after imaging to confirm that negligible loss of solvent had occurred during imaging. Images were reconstructed to a matrix size of $256 \times 256 \times 8$ data points.

2.4. Dynamic mechanical analysis

Dynamic mechanical analysis was performed using a Rheometric Scientific MK II DMTA in the bending mode with dual cantilever. Rectangular specimens measuring $25 \times 10 \times 1$ mm^3 were scanned at 1 Hz in the temperature scan mode. The main parameters determined were tan δ and loss modulus E''. The glass transition temperature was defined as the temperature corresponding to the tan δ peak maximum.

2.5. Differential scanning calorimetry

The glass transition temperature of TPI specimens was

determined by a computer controlled Perkin–Elmer DSC 7. Samples were heated directly from ambient to determine the T_g, which was taken as the mid-point of the heat capacity change.

2.6. Wide angle X-ray scattering

Wide angle X-ray scattering (WAXS) was carried out on a Rigaku Geigerflex generator with an accelerating voltage of 30 kV and a current of 30 mA supplied by Ni filtered Cu-Kα radiation. Data were acquired in transmission mode from $2\theta = 3$–$50°$ in intervals of 0.05°.

2.7. Mechanical testing

Tensile tests were carried out on a Minimat testing machine (Rheometric Scientific, USA) on dumb-bell shaped specimens cut from compression moulded sheets. The gauge length was 30 mm and the crosshead speed was 0.2 mm/min. Two types of ESC experiments were carried out: (1) the upper surface of specimens was fully covered with solvent throughout the test using a small pipette; and (2) the upper surface of specimens was fully covered with solvent using a small pipette after yielding and neck formation occurred.

3. Results and discussion

3.1. Gravimetric diffusion studies

The progress of the diffusion of various solvents into amorphous TPI was observed from the weight increase with root time, at room temperature, as shown in Fig. 1. The greatest increase in weight occurred in the early stages of immersion and this was followed by a progressive decrease in the rate of uptake until equilibrium was reached and the weight remained constant with time. Equilibrium was reached after a period varying between hours and weeks, depending on the solvent. The non-Fickian kinetics of the weight increase for each solvent, with the exception of acetone, can be seen from the plots. A change in slope of the weight uptake curve for chloroform and dichloromethane occurred at around 100 h. This was ascribed to the meeting of the solvent fronts at the centre of the sample resulting in the release of swelling stresses, changes in sample dimensions and an increase in the rate of diffusion [20]. The kinetics of solvent uptake were analysed in the initial stages of diffusion according to Fick's second law for one-dimensional diffusion:

$$\frac{\partial c}{\partial t} = D\frac{\partial^2 c}{\partial x^2} \tag{1}$$

where c is the concentration, t the time, x a point along the axis and D the diffusion constant. For a plane sheet of thickness h the diffusion constant D was evaluated in the initial stages by:

$$\frac{W_t}{W_e} = \left(\frac{4D^{1/2}}{\pi^{1/2}h}\right)t^{1/2} \tag{2}$$

where W_t and W_e are the weight increase at time t and at equilibrium, respectively. The diffusion constant was determined from the slope of plots of W_t/W_e against $t^{1/2}$ and only acetone showed a linear dependence. The weight increase according to one-dimensional Fickian diffusion was also simulated using the experimental value of the diffusion coefficient for chloroform, with time ranging from 1 to 1280 h. The results were plotted in Fig. 2 as normalised weight increase against film thickness and the profiles were similar to those previously reported by Crank [21]. The solvent fronts are predicted to meet at the centre of the sample after 56 h. The discrepancy between the predicted and experimental gravimetric data arose because of the non-Fickian diffusion of chloroform in TPI.

The diffusion of low molecular weight substances into glassy polymers does not always obey Fick's laws of diffusion. Deviations from Fickian diffusion are a consequence of the finite rate at which the polymer structure changes during the diffusion process, and this is strongly dependent on temperature and crystallinity, if the polymer is susceptible to solvent-induced crystallisation. The various types of diffusion outlined by Alfrey et al. [22], were determined from

$$\frac{W_t}{W_e} = kt^n \tag{3}$$

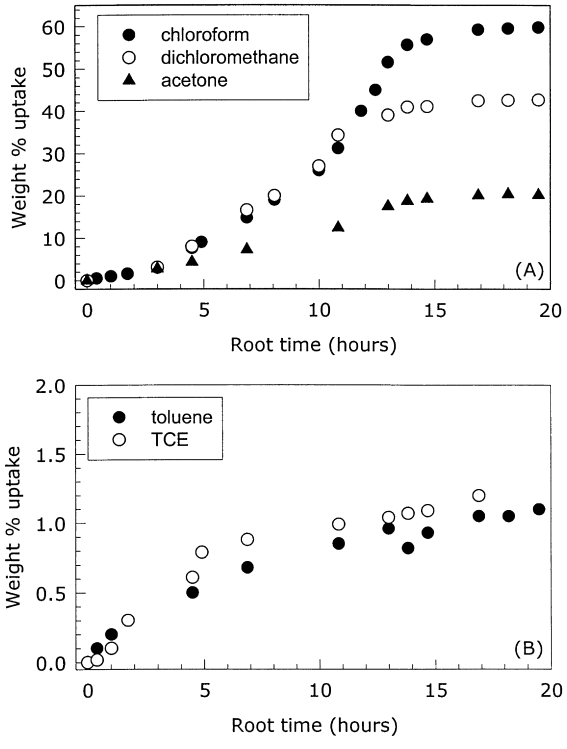

Fig. 1. Weight uptake of solvents by TPI.

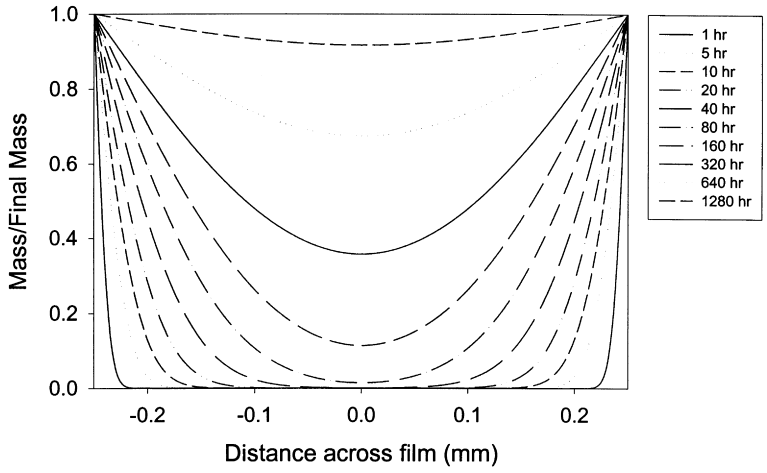

Fig. 2. Solvent diffusion into TPI film of 0.5 mm thickness calculated assuming one-dimensional Fickian diffusion. D was the experimental value for chloroform of 15×10^{-11} cm^2 s^{-1} and time ranged from 1 to 1280 h.

with k and n as constants. If $n = 1/2$ the diffusion was classified as Fickian (case I); if $n = 1$ the diffusion was case II and if n was between 1/2 and 1 the diffusion was case III. Log–log plots based on Eq. (3) were generally linear and the exponent n was determined from the slope. Solvent uptake at equilibrium, diffusion constant D and n values for diffusion of various solvents into amorphous TPI are listed in Table 1. A feature of the equilibrium uptake of the chlorinated solvents is that while chloroform and dichloromethane were absorbed in significant amounts, only 1.4 wt% of TCE diffused into the polymer. It was interesting to compare this with previous findings concerned with solvent uptake by aromatic thermoplastics, the majority of which focused on PEEK. It was reported that amorphous PEEK absorbed 51.2 wt% of chloroform and 36 wt% of dichloromethane [23]. The uptake of these solvents was accompanied by plasticisation and crystallisation which both have a major, and sometimes undesirable, effect on the mechanical behaviour of PEEK. Other works [24] showed that amorphous PEEK absorbed greater than 200 wt% of TCE. Strong Lewis acid–base interactions were postulated as the likely explanation for this with the carbonyl, ether and aromatic groups in PEEK acting as electron donors and TCE acting as an electron acceptor.

Table 1
Solvent uptake at equilibrium, diffusion constant and n values for diffusion of solvents into amorphous TPI

Sample	Equilibrium uptake (wt%)	D (10^{-11} cm^2 s^{-1})	n
Chloroform	60	15.0 ± 0.25	0.68 ± 0.02
Dichloromethane	43	5.61 ± 0.28	0.72 ± 0.02
Acetone	20	3.72 ± 0.02	0.56 ± 0.03
TCE	1.4	0.0036 ± 0.0005	0.24 ± 0.02
Toluene	1.1	0.0029 ± 0.0004	0.25 ± 0.01

The fact that only a small quantity of TCE diffused into TPI suggested other factors were important in influencing solvent uptake. In particular, the larger size of the TCE molecules may have prevented significant uptake by TPI, while the packing of TPI chains was also important. The diffusion constant increased with increasing equilibrium uptake but, even for chloroform, the rate of solvent uptake was significantly lower than that of PEEK when immersed in similar solvents [25]. According to the values of n the kinetics of acetone diffusion into TPI were consistent with Fickian diffusion, chloroform and dichloromethane followed case II diffusion while the uptake of toluene and TCE followed a low power dependence on time. Hence, Eq. (2) was not a valid description of solvent diffusion in TPI of the solvents studied, with the exception of acetone. The diffusion of solvents into amorphous PEEK was frequently reported to observe case II kinetics [26]. Thermally crystallised TPI was also immersed in each solvent and it was found that the maximum equilibrium uptake occurred with chloroform and was less than 1 wt%. Comparison of the behaviour of TPI with that of PEEK is useful because the interaction of PEEK with solvents has been studied extensively and the two polymers share structural and morphological characteristics.

3.2. NMR imaging

In recent years the technique of NMR imaging has proved a useful adjunct to measurements of mass uptake of solvents by polymers. The method provides a two- or three-dimensional map of the distribution of solvent molecules within the polymer at any selected time during ingress. The polymer is removed from the solvent and an NMR image acquired over a time that is short compared with the total time taken for diffusion of the solvent into the polymer. In the acetone/TPI system studied in this work such a requirement was easily met, however, difficulties

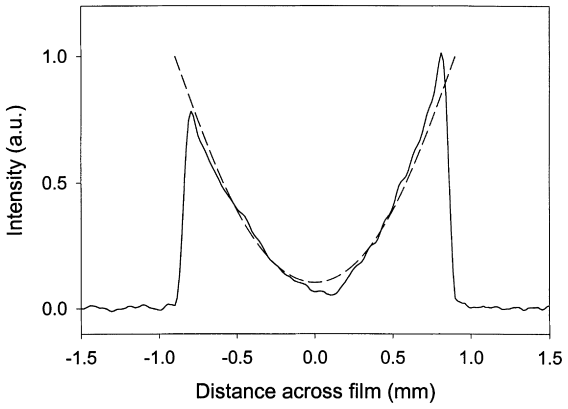

Fig. 3. The distribution of acetone across TPI measured by NMR imaging (solid line). The dashed line was a fit of the data to the solution of Fick's second law for diffusion into cylinders.

may arise in systems which swell rapidly, for example with strongly hydrophilic polymers in water.

The frequency of the NMR signal depends on the strength of the applied magnetic field, and so if a linear gradient in magnetic field is applied across an object, the NMR frequency of the proton nuclei within the object becomes dependent on position along the plane of the gradient. In principal, gradients can be applied in all three Cartesian dimensions and a three-dimensional image thus obtained, however, in practice a two-dimensional image of a slice through an object is acquired with the aid of slice selective radio frequency pulses. The image is usually acquired using a spin-echo pulse sequence, so that the amplitude of the image at each point in space depends on the spin–spin relaxation times (T_2) of the proton nuclei. In many solvent/polymer systems the T_2 of the polymer is of the order of 10–100 μs, while that of the solvent may be 10–100 ms. Since the minimum echo time achievable on commercial equipment is of the order of 1–10 ms, the protons of the polymer do not contribute to the intensity of the image, and the image results from signal from the solvent only. From the above discussion it is apparent that the form of the image will only reflect the distribution of solvent molecules if either the T_2 relaxation times of the solvent are constant across the polymer, or are long compared with the echo time. Care must therefore be taken to ensure that such conditions are met with each polymer/solvent system, especially those where strong interactions occur between the polymer and solvent molecules.

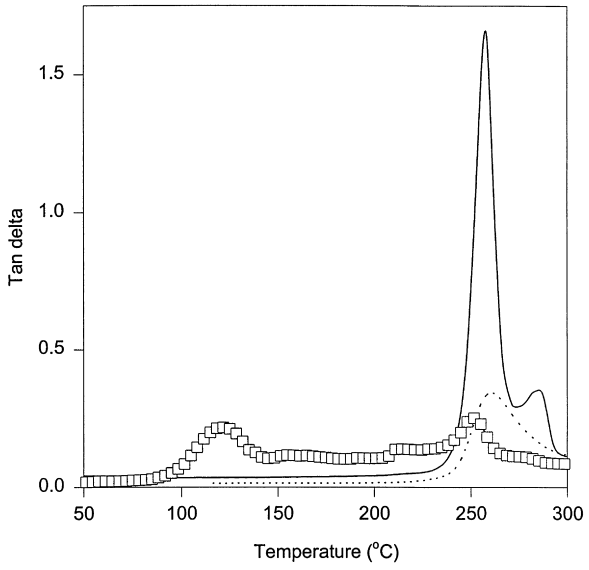

Fig. 4. Dynamic mechanical analysis of TPI: (—) amorphous TPI; (– – – –) crystalline TPI; (□) TPI immersed in chloroform for 4 weeks at room temperature.

Fig. 3 shows a plot of the distribution of acetone across the TPI sheet measured by NMR imaging. The total diffusion time prior to imaging was 190 days. It is apparent that during handling of the sample solvent was lost from the upper 0.1 mm of the surface; however, this had no effect on the analysis of the underlying profile. The dashed line was a fit of the data to the solution of Fick's second law for diffusion into cylinders [27]. It can be clearly seen that the image intensity was well described by Fick's law; the value of diffusion coefficient obtained from this analysis was 6.5×10^{-11} cm^2 s^{-1}.

3.3. Solvent plasticisation of TPI

The solvent plasticisation of glassy thermoplastics and subsequent solvent induced crystallisation has been well documented in the literature [28]. In many cases solvent uptake leads to swelling of the polymer, loss of mechanical properties and ultimate failure. Crystallisation occurs as a result of a lowering of the T_g by the solvent to room temperature or below. Dynamic mechanical loss data for untreated amorphous and semi-crystalline TPI and amorphous TPI after immersion in chloroform for a period of 4 weeks are shown in Fig. 4. The behaviour of untreated TPI was typical of thermoplastics, with the amorphous specimen showing a strong, narrow T_g (at 258°C) and post-T_g crystallisation, while the semi-crystalline TPI had a broad and weak T_g at 262°C and showed no evidence of further crystallisation. For the immersed specimen the T_g at 122°C was due to plasticisation by chloroform, although at this temperature an estimated 20 wt% of the solvent had already been lost from the specimen. On further heating additional solvent was lost and a second weak T_g was seen at 252°C, indicating that the majority of the chloroform had, by this stage, desorbed from the specimen. Crystallisation was also observed to occur in this specimen during heating by the gradual development of opacity. The dynamic mechanical behaviour of untreated and plasticised TPI was qualitatively very similar to that previously reported for PEEK [29].

3.4. Solvent-induced crystallisation

Much research has been conducted in recent years on the

crystallisation of semi-crystalline TPI. Okuyama et al. [30] determined the unit cell of oriented films of TPI to be orthorhombic with dimensions of $a = 7.89$ Å, $b = 6.29$ Å and c(fibre axis) $= 25.11$ Å. The unit cell was found to contain two polymer chains with a 1/1-helical symmetry. The molecular conformation of TPI was investigated, which showed four degrees of freedom about the ether linkages and which accounted for the comparatively lower melting temperature of TPI. The overall chain conformation of TPI was straight and close to the fully extended conformation.

Friler et al. [31] conducted an extensive study on the crystalline morphology of TPI using DSC, WAXS and SAXS and indicated that the crystals to be only a few molecular repeat units thick with an alternating crystalline-amorphous periodic structure. Takahahsi et al. [32] solvent cast and annealed films of TPI and studied the crystal structure using electron microscopy and wide-angle X-ray spectroscopy. Electron microscopy indicated the crystal thickness to be approximately 130 Å. The authors concluded that TPI formed folded-chain crystals.

The WAXS pattern of TPI quenched from the melt in iced water (Fig. 5A) indicated that the polyimide was fully amorphous. A broad maximum centred at $2\theta = 5°$ was clearly seen which corresponded to 17.7 Å. This length was close to the c period reflection (001) (Fig. 5B) of 25.4 Å indicating an alignment of amorphous segments along the chain axis. Friler et al. showed this alignment to reduce upon annealing above the T_g.

Crystalline diffraction peaks were observed in TPI that had been annealed at 290°C for 2 h. Applying Scherer's Law [33] to the scattering peak (110) at $2\theta = 18°$, gave an average crystalline particle thickness of 69 Å. This corresponded to approximately two to three polymer chains. This length was approximately half the crystal thickness determined by Takahashi et al.; however the TPI in their study was cast from solution. Applying a similar analysis on the (001) reflection indicated a particle length of 125 Å that corresponded to five repeat units per particle. The WAXS scan of solvent exposed TPI (Fig. 5C), with its close correspondence to the pattern of amorphous TPI, showed that chloroform did not cause sufficient plasticisation of TPI for crystallisation to occur. The T_g of TPI containing an equilibrium amount of chloroform was estimated, using the Fox equation, to be 66°C, indicating that the polymer was in the glass state at room temperature and would therefore not crystallise.

This result was supported by DSC studies, the results of which are presented in Fig. 6. Amorphous, untreated TPI (curve A) displayed typical thermoplastic behaviour with a T_g around 250°C, followed by crystallisation and melting. A scan of TPI immersed in chloroform for 4 weeks followed by drying under vacuum at 220°C for 2 weeks showed the effect of residual solvent on thermal behaviour (curve B). The T_g was slightly lowered through plasticisation by the remaining solvent and was hidden under the physical ageing peak around 249°C, while crystallisation and melting both occurred at significantly reduced temperatures, compared with amorphous TPI. By contrast, a comparison of the thermal characteristics of the specimen shown in curve C to amorphous TPI showed that the solvent was almost completely removed by heating in the DSC at a temperature above the glass transition but below the minimum isothermal crystallisation temperature (255°C). The similar form of each scan and the strong crystallisation exotherm present in curve C during heating suggested that crystallisation did not occur during immersion in chloroform at room temperature.

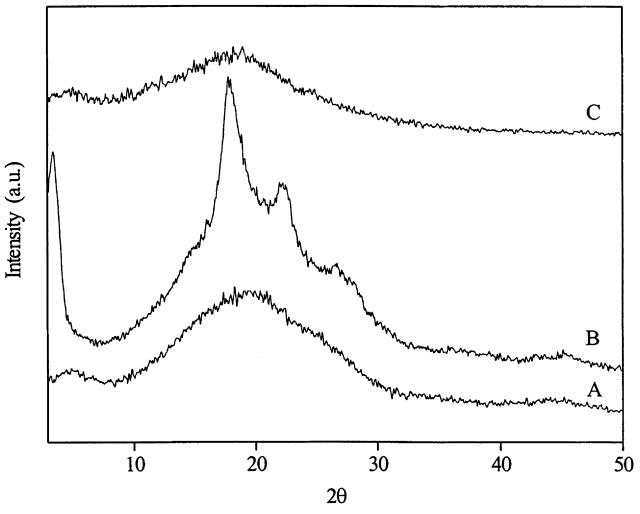

Fig. 5. Wide-angle X-ray scattering of TPI: (A) TPI quenched from the melt in iced water; (B) thermally crystallised TPI; and (C) TPI immersed in chloroform for 4 weeks at room temperature.

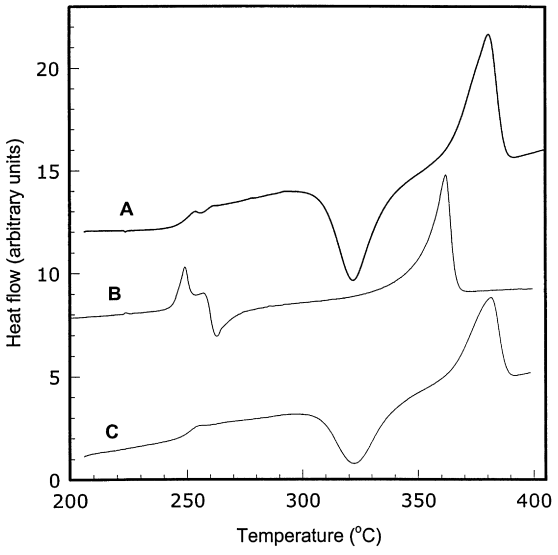

Fig. 6. DSC of TPI: (A) amorphous TPI; (B) TPI immersed in chloroform for 4 weeks at room temperature and then stored under vacuum at 220°C for 2 weeks; and (C) TPI immersed in chloroform for 4 weeks at room temperature and then stored in the DSC at 255°C for 2 h.

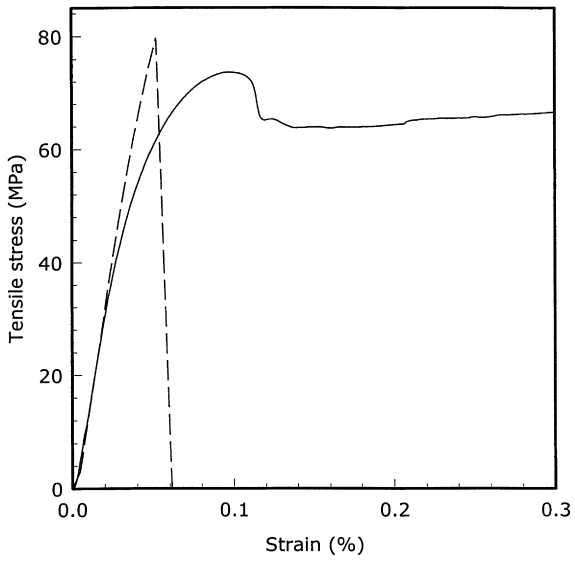

Fig. 7. TPI mechanical behaviour. (—) amorphous TPI. (– – – –) crystalline TPI.

3.5. ESC behaviour

Load–displacement curves for amorphous and semi-crystalline TPI are shown in Fig. 7. The amorphous specimen yielded and formed a stable neck under load in a manner typical of a ductile thermoplastic. The yield stress, defined as the point of maximum load, was 73.3 ± 1.3 MPa, and the drawing stress was approximately 65 MPa. The semi-crystalline specimen did not form a neck and underwent brittle failure at low strain. The maximum stress was 79.7 ± 0.9 MPa.

Fig. 8 shows the load–displacement behaviour of amorphous TPI with the upper surface of the specimen covered with solvent throughout the test. In the presence of toluene and acetone crazes formed as yielding and neck formation occurred and this was followed by propagation of the neck at constant stress and further craze formation until failure occurred. These solvents caused yielding and load drop to occur at a lower stress value and over a narrow strain range, compared with untreated TPI, and the corresponding drawing stress was also reduced. Removal of toluene from the specimen surface resulted in an increase in load. This resulted from the increase in T_g after partial solvent loss from the polymer matrix, and the orientation of polymer chains along the long axis of the specimen during tensile drawing, raising the strength. Both effects combined to overcome the loss in strength caused by craze formation. It is worth noting that the increased load was borne by a smaller cross-section of specimen. Failure of the specimen occurred when crazes combined at higher strain to form a crack that propagated rapidly across the width of the specimen. Acetone permitted necking and drawing to occur prior to failure while chloroform caused crazes to form around the point of maximum load, with crack formation and failure occurring soon afterwards. A neck did not form. Coverage of the surface of a semi-crystalline TPI specimen by each solvent caused relatively rapid failure at low strain (Fig. 9) accompanied by the formation of fewer crazes, compared with the amorphous case.

Tensile yield stress values for amorphous and crystalline TPI specimens covered by solvent are listed in Table 2. The magnitude of the reduction in yield stress, compared with untreated TPI, was greater for amorphous specimens and was proportional to the uptake of solvent by TPI, while chloroform caused the greatest reduction. Although crystalline TPI absorbed less than 1 wt% of chloroform this reduced the yield stress by almost 80%. The lower solvent

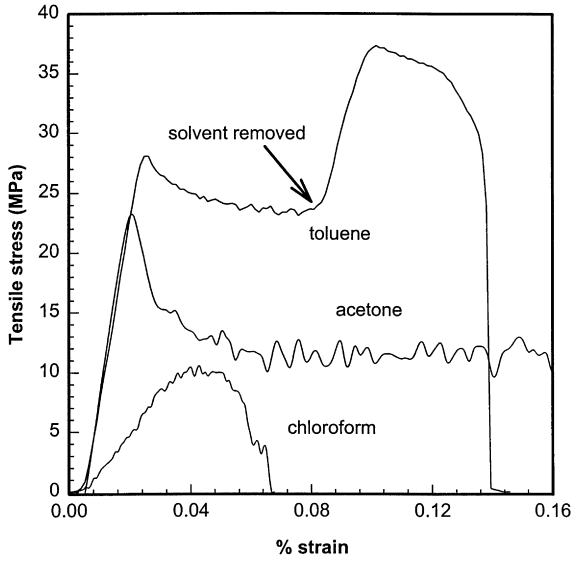

Fig. 8. Mechanical behaviour of amorphous TPI with the upper surface of the specimen covered by solvent throughout the test, except where indicated in the case of toluene.

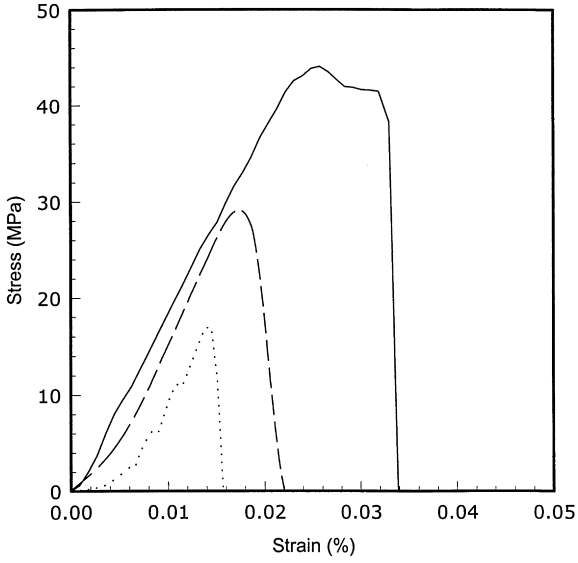

Fig. 9. Mechanical behaviour of crystalline TPI with the upper surface of the specimen covered by solvent throughout the test. (—) toluene. (– – – –) acetone. (· · · · · ·) chloroform.

Table 2
Tensile yield stress values for amorphous and crystalline TPI with the upper surface of the specimen covered by solvent throughout the test

	Yield stress (MPa)/ amorphous TPI	Yield stress (MPa)/ crystalline TPI
Toluene	28	44
Acetone	23	29
Chloroform	10	17

uptake of crystalline TPI was due to the reduced amorphous volume and close packing of the crystalline chains that were very effective in blocking the passage of mobile solvent molecules. The small quantity of solvent that was absorbed was concentrated in the amorphous phase and, combined with the inherent brittle nature of crystalline TPI, was able to promote failure at a relatively low stress.

Tensile experiments were also carried out in which solvent was added to the upper surface of an untreated TPI specimen being drawn at constant stress. Addition of solvent along the gauge length of semi-crystalline TPI caused rapid failure, and few crazes were formed. Addition of a constant quantity of solvent to the undrawn region of amorphous TPI caused a significant load drop (Fig. 10) and formation of crazes. Removal of the solvent produced a load recovery close to the untreated drawing stress. In this case the extent of plasticisation was not as great as that indicated by Fig. 8, since each solvent was in contact with the specimen for a shorter time and therefore less ingress occurred.

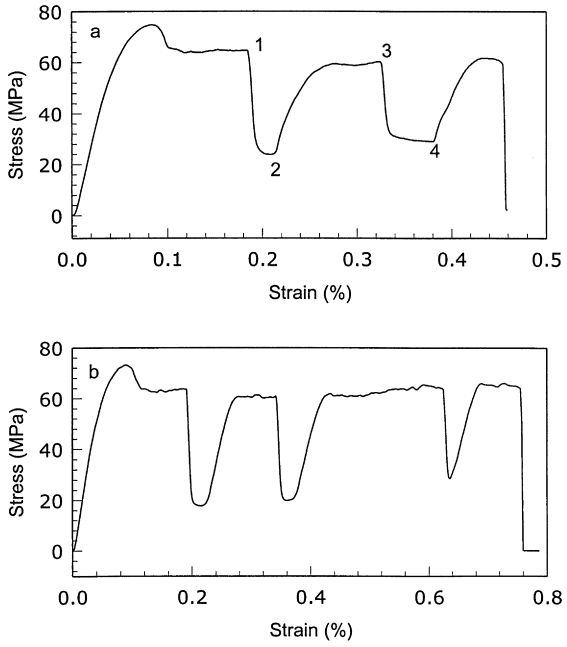

Fig. 10. Mechanical behaviour of amorphous TPI with addition and removal of solvent from the upper surface of the specimen as indicated: (a) (1) acetone added, (2) acetone removed, (3) toluene added, (4) toluene removed; and (b) repeated addition and removal of chloroform.

These observations were a direct consequence of the solvent plasticisation of TPI and were a measure of the susceptibility of TPI to environmental stress cracking. Thus, the magnitude of the load drop and the number of crazes formed were directly related to the affinity of the solvent for TPI. The load was considered to drop to the critical value for craze formation which was 18 MPa for chloroform, 24 MPa for acetone and 29 MPa for toluene, confirming that chloroform is the more aggressive ESC agent for TPI and toluene the least aggressive. The relationships between plasticisation, craze formation and mechanical behaviour of thermoplastic polymers were addressed by Volynskii and Bakeev in a recent review [34].

4. Conclusions

Amorphous TPI absorbed significant amounts of certain solvents, resulting in plasticisation, in line with the behaviour of other amorphous aromatic thermoplastics. However, the high T_g of TPI in the untreated state prevented solvent-induced crystallisation occurring during room temperature immersion. The diffusion coefficient for acetone absorption was in reasonable agreement when measured by the different techniques of weight uptake and NMR imaging. The difference is explained by the different residual stress in each specimen resulting from the rapid cooling during sample preparation. The faster quenching rate of the thinner gravimetric specimen produced higher residual stress and therefore a higher diffusion constant, compared with the thicker NMR specimen, as the rate of solvent absorption of polymers is known to be proportional to the imposed or residual stress. It was confirmed that the conditions for ESC of a thermoplastic polymer to occur were internal or external stress in combination with a sensitising agent, such as a liquid. The mechanical behaviour of TPI was altered by exposure to solvent, and in particular the tensile yield stress and drawing stress of amorphous TPI were lowered. The reduction is related to the affinity of solvent for TPI. Crystalline TPI failed in tension in a brittle fashion in both the untreated and solvent-exposed state, although it did not undergo such a large reduction in yield stress, compared with amorphous TPI. Crystalline TPI formed fewer crazes on exposure to solvent.

References

[1] Hergenrother PM. SPE Conference on High Temperature Polymers and their Uses, Case Western, October 1989.
[2] Okuyama K, Sakaitani H, Arikawa H. Macromolecules 1992;25:7261.
[3] Huo PP, Cebe P. Coll Polym Sci 1992;270:840.
[4] Burford RP, Benson CM. Mats Forum 1995;19:129.
[5] Weisenberger LA, Koenig JL. J Polym Sci Polym Lett Ed 1989;27:55.
[6] Weisenberger LA, Koenig JL. Appl Spectrosc 1989;43:1117.
[7] Weisenberger LA, Koenig JL. Macromolecules 1990;23:2445.
[8] Grinsted RA, Koenig JL. Macromolecules 1992;25:1235.

[9] Lloyd CH, Scrimgeour SN, Chudek JA, Hunter G, Mackay RL. Plast Rubber Comp Proc Appl 1995;24:181.
[10] Ercken M, Adriaenses P, Reggers G, Carleer R, Vanderzande D, Gelan J. Macromolecules 1996;29:5671.
[11] Webb AG, Hall LD. Polym Commun 1990;31:422.
[12] Webb AG, Hall LD. Polym Commun 1990;31:425.
[13] Webb AG, Hall LD. Polymer 1991;32:2926.
[14] Ghi P, Hill DJT, Maillet D, Whittaker AK. Polym Commun 1996;38:3985.
[15] Ilg M, Pfleiderer B, Albert K, Rapp W, Beyer E. Macromolecules 1994;27:2778.
[16] Ercken M, Adriaenses P, Vanderzande D, Gelan J. Macromolecules 1995;28:8541.
[17] Grinsted RA, Koenig JL. Macromolecules 1992;25:1229.
[18] Hyde TM, Gladden LF, Mackley MR, Gao P. J Polym Sci Polym Chem Ed 1995;33:1795.
[19] Ercken M, Adriaenses P, Vanderzande D, Gelan J. Macromolecules 1995;28:8541.
[20] Gehrke SH, Biren D, Hopkins JJ. J Biomater Sci Polym Engng 1994;6:375.
[21] Crank J. The Mathematics of diffusion. 2nd ed.. Oxford: Clarendon Press, 1975.
[22] Alfrey T, Gurnee EF, Lloyd WG. J Polym Sci C 1966;12:249.
[23] Wolf CJ, Bornmann JA, Grayson MA, Anderson DP. J Polym Sci B 1992;30:251.
[24] Stuart BH, Williams DR. Polymer 1994;35:1326.
[25] Hay JN, Kemmish DJ. Polymer 1988;29:613.
[26] Mensitieri G. Del Nobile MA, Apicella A, Nicolais L. Polym Engng Sci 1989;29:1786.
[27] Carslaw HS, Jaeger JC. Conduction of heat in solids. 2nd ed.. Oxford: Clarendon Press, 1959 (p. 199).
[28] Cornelis H, Kander G. Polymer 1996;37:5627.
[29] Barton JM, Goodwin AA, Hay JN, Lloyd JR. Polymer 1991;32:260.
[30] Okuyama K, Sakaitani H, Arikawa H. J Macromol Sci-Phys 1994;B33(1):75.
[31] Friler JB, Cebe P. Polym Engng Sci 1993;33:587.
[32] Takahashi T, Yuasa S, Tsuji M, Sakurai K. J Macromol Sci Phys B 1994;33(1):63.
[33] Alexander LE. X-ray diffraction methods in polymer science. New York: Wiley, 1969.
[34] Volynskii AL, Bakeev NF. Solvent crazing in polymers, Studies in polymer science, vol. 13. Amsterdam: Elsevier, 1995.